Journal of Solid Mechanics Vol. 9, No. 4 (2017) pp. 811-820

Numerical and Experimental Study on Ratcheting Behavior of Plates with Circular Cutouts under Cyclic Axial Loading

K. Kolasangiani [1], M. Shariati [1,*], Kh. Farhangdoost [1], A. Varvani-Farahani [2]

[1] *Department of Mechanical Engineering, Ferdowsi University of Mashhad, Mashhad, Iran*
[2] *Department of Mechanicaland and Industrial Engineering, Ryerson University, Toronto, Canada*

Received 26 July 2017; accepted 29 September 2017

ABSTRACT

In this paper, accumulation of plastic deformation of AISI 1045 steel plates with circular cutouts under cyclic axial loading is studied. Loading was applied under force-control conditions. Experimental tests were performed using a Zwick/Roell servo hydraulic machine. Under force-control loading with nonzero mean force, plastic strain was accumulated in continuous cycles called ratcheting. Numerical analysis was carried out by ABAQUS software using nonlinear isotropic/kinematic hardening model. The results of the numerical simulations were compared to experimental data. The results demonstrated that the ratcheting response of plates with circular cutouts could be numerically simulated with a reasonable accuracy. It was observed that the local and global plastic deformation increase with increasing the notch diameter. Also, maximum principal stress was the main parameter for initiation of crack around the notch. Based on numerical results, at notch root, both ratcheting strain and local mean stress relaxation was occur simultaneously and due to relaxation of local mean stress, plastic shakedown was occurred.

Keywords : Plate with circular cutout; Numerical and experimental study; Cyclic loading; Nonlinear isotropic/kinematic hardening model.

1 INTRODUCTION

STRUCTURE components are often subjected to cyclic loading. A cyclic accumulation of plastic deformation will occur in the components when a cyclic loading with nonzero mean stress under force-control condition is applied. Although the plastic strain in a cyclic loading might be low, their accumulation in one direction during loading is considerable. This phenomena is known as cyclic plasticity or ratcheting. Moreover, the engineering components contain notches like grooves, holes, etc. An existence of notch or geometrical discontinuity is necessary for mechanical connection that it is effective in degradation of life. When a component is loaded, a stress concentration and severe plastic deformation appear at notch root. The ratcheting as a secondary phenomena of cyclic plasticity can accelerate fatigue damage or even act as the failure mechanism itself. So, local plastic strain with global accumulation of plastic deformation are intensify crack initiation and its growth around the notch to failure occur. Therefore, study of cyclic behavior of notched specimens and determination of the stress-strain state at critical locations is a prerequisite to the design and analysis of structures containing stress concentration. The issue of the local stress/strain at notch root under cyclic loading has been studied seriously for the past years [1-8].

[*]Corresponding author. Tel.: Tel.: +98 511 880 5159; Fax: +98 511 880 6055.
E-mail address: mshariati44@um.ac.ir (M.Shariati).

Savaidis et al [9] performed on elastic-plastic finite element analysis for a notched shaft subjected to cyclic loading. They observed both the stress amplitude and the mean stress have effects on the local elastic-plastic stress-strain response at the notch root by using von Mises yield criterion and the kinematic hardening rule of Prager/Ziegler. Wang and Rose [10] studied the transient and steady-state cyclic deformation behavior at notch root. They found that both elastic-perfectly plastic and linear kinematic hardening models predict an immediate plastic shakedown while nonlinear kinematic hardening law predicts a progressive shakedown. Fatigue behavior of DZ125 solidified super alloy with single-edge notched were tested by Shi et al [11]. They observed that the ratcheting is affected by both stress concentration factor and the nominal stress. Also, they indicated the cracking occurs at the location where the maximum principal stress is the highest.

In this investigation, ratcheting behavior of AISI 1045 plates with circular cutouts under cyclic loading is studied, using experimental tests and compared to numerical results. Under force-control condition, global accumulation of plastic deformation was observed. Also, the numerical results show the combined ratcheting and mean stress relaxation at the notch root.

2 EXPERIMENTAL TESTS

2.1 Specimens' specification

The material used in this work is AISI 1045 steel plate. The chemical compositions of the material are listed in Table 1. To determine the mechanical properties of AISI 1045, simple and standard tension test were performed according to ASTME A370-05 standard [12]. The obtained results are shown in Table 2.

Table 1
Chemical compositions of AISI 1045 steel.

C	Mn	Si	Ni	S	P	Cr	Fe
0.445	0.56	0.261	0.085	0.005	0.017	0.123	98.3
Mo	Al	Cu	Co	Pb	Nb	V	W
0.006	0.02	0.142	0.004	<0.001	<0.001	<0.001	<0.007
N							
0.007							

Table 2
Mechanical properties of plate.

Yield stress (*MPa*)	Modulus elasticity (*GPa*)	Ultimate stress (*MPa*)	Failure strain
324	203	564	0.13

2.2 Test device and boundary conditions

Experimental tests in this study have been performed by using Zwick/Roell servo hydraulic machine (Fig. 1). This device can be loaded to 100*kN* dynamically.

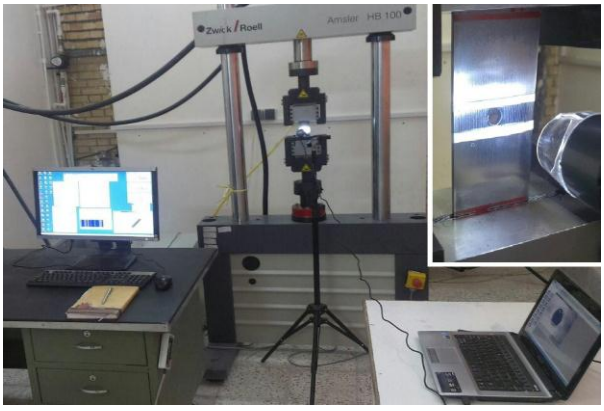

Fig.1
Zwick/Roell servo hydraulic machine.

Geometric dimensions and boundary conditions of plates with circular cutouts are shown in Fig. 2. Lower plate was clamped and the cyclic force was applied through a device jaw at the upper edge of the plate. A Dino light camera was used to view the crack initiation and crack propagation around the notch at maximum magnification of 200 times. The camera has the ability to capture in any cycles by measuring the crack length and crack angle.

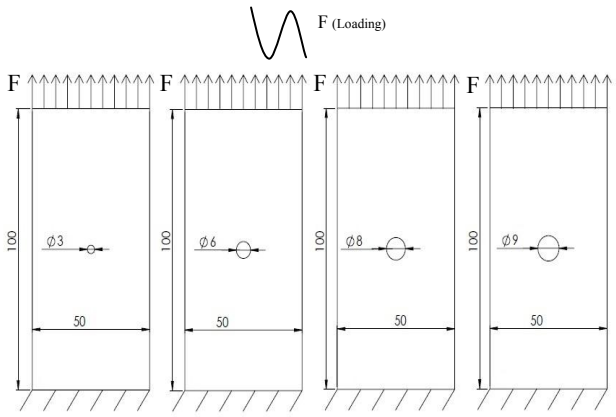

Fig. 2
Geometric dimensions and boundary conditions of plates with circular cutouts (dimensions are in millimeter).

2.3 Experimental results

All tests were performed in the force-controlled condition and any specimens subjected to cyclic loading with mean force and force amplitude of 25*kN*. Loading rate of all tests was 50*kN/s*. In this research, the ratcheting displacement will be defined as the maximum displacement of each cycle.

2.3.1 Ratcheting analysis

The force-displacement hysteresis loops under unsymmetrical cyclic loading are not closed. Due to unclosed hysteresis loops and shifting of the loops under cyclic loading, accumulation of plastic deformation or ratcheting occur. Fig. 3 shows the hysteresis loops for plate with notch diameter of 3*mm* under unsymmetrical force-control condition. Loading is applied as long as the failure of the sample occurs. Speed of hysteresis curve movement decreases at first and finally increases until the failure occurs.

According to Fig. 4, ratcheting displacement increases but its rate reduces at first and finally increases to failure of the plate with circular cutout. Transient point is defined a point located between the area with a high ratcheting displacement rate and an area with constant ratcheting displacement rate to differentiate transient ratcheting and continuous ratcheting [13]. So, it is possible to define two transition points as the first and the second points for a plate with circular cutout which divides its curve into the three areas [14].

The decrease in the ratcheting displacement rate can be explained by the formation and distribution of dislocations associated with cyclic deformation. When a material is subjected to cyclic deformation, dislocations in its structure are created by strain hardening. These dislocations were initially placed in chaotic state, then by increase in the number of cycle, they turn into the elements of orderly dislocation and this lead to reduction of ratcheting displacement rate [15].

By comparing the ratcheting displacement of plates with different notch diameters, it can be seen that the ratcheting displacement increases with increasing the notch diameter. The ratcheting displacement or accumulation of plastic deformation can be two parts that are local part around the notch and nominal part away from the notch. As the geometric dimensions of the specimens are the same, the nominal part is the same under the same loading. So, local part, which is controlled by stress concentration and nominal stress in net section, is the main parameter for increasing of plastic deformation. Stress concentration decreases and nominal stress in net section increases by increment of notch diameters. Therefore, based on the experimental results, the nominal stress in net section can be regarded as a key parameter to dominate discrepancy in plastic deformation between plates with different notch diameters. Also, by increasing the notch diameter of the plate, the first and second transition points occur in fewer cycles but ratcheting displacements in these points increase. So, first and second transition points occur faster with higher maximum axial stress at notch root.

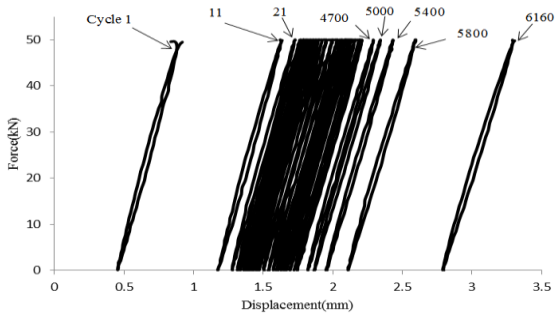

Fig.3
Experimental ratcheting behavior of plate with notch diameter of 3*mm*.

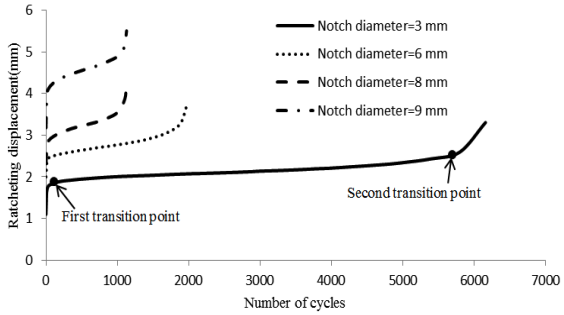

Fig.4
Experimental ratcheting displacement for plates with different notch diameter.

2.3.2 Crack initiation and propagation

The crack initiation and the following crack growth phenomena for plates with circular cutouts were observed at any cycle by Dino light camera, as shown in Figs. 5 and 6. The results reveal that cracks usually initiate around the notch root. Also, the crack paths on two sides of notch may be inclined line. Material microstructure and defects affects the crack propagation.

Fig. 7 presents the main crack length with the increase of number of cycles. It can be seen that the main crack propagate slowly at first and gradually, the speed of crack growth increases. Also, it is shown that the crack growth rate is higher for specimen with larger notch diameter. As said in previous, based on experimental results, nominal stress in net section is the main reason to crack growths faster.

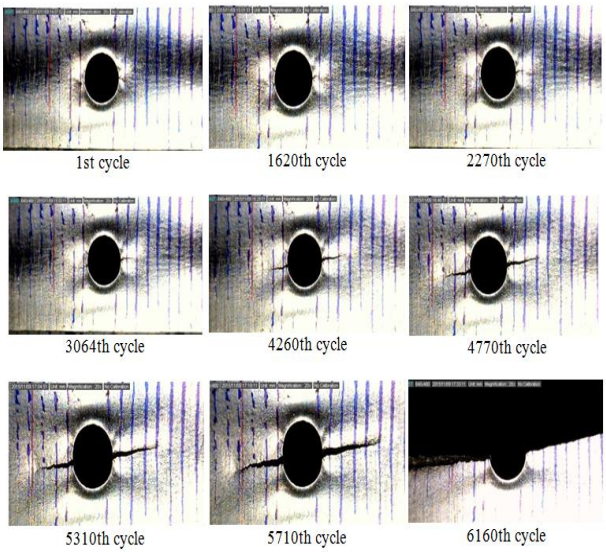

Fig.5
Crack initiation and propagation of specimen with notch diameter of 3*mm* in experimental tests.

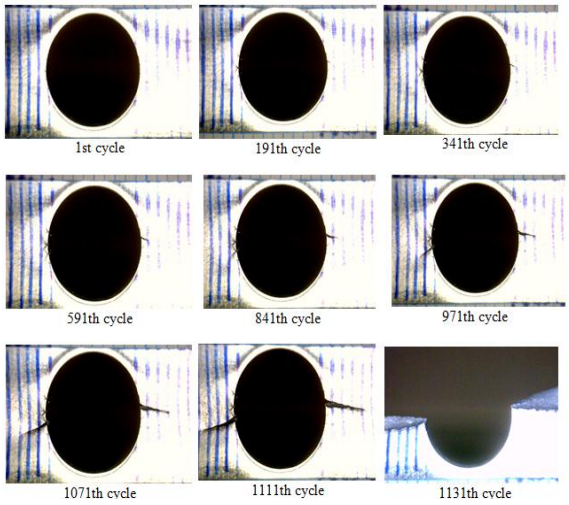

Fig.6
Crack initiation and propagation of specimen with notch diameter of 9*mm* in experimental tests.

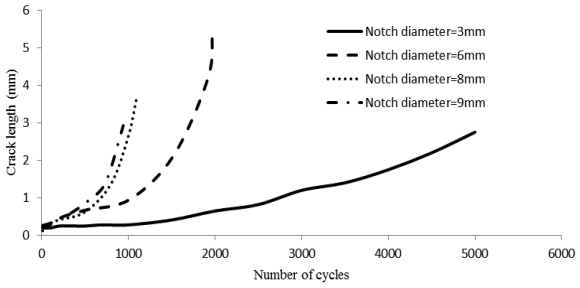

Fig.7
Relationships between the main crack length and cycles for the plates with different notch diameter in experimental tests.

3 NUMERICAL ANALYSIS

The numerical simulations were carried out using the finite element software ABAQUS. This software between most ability, can be used for metals subjected to cyclic loading to analyze by a kinematic hardening model with two parts, linear kinematic and nonlinear isotropic/kinematic hardening. The linear kinematic hardening model has a constant hardening modulus, and the nonlinear isotropic/kinematic hardening model has both nonlinear kinematic and nonlinear isotropic hardening components.

The evolution law of a linear kinematic hardening component describes the translation of the yield surface in stress space through the backstress, α. When temperature dependence is omitted, this evolution law is the linear Ziegler hardening law according to Eq. (1) [16].

$$\alpha = C\frac{1}{\sigma^0}(\sigma_{ij} - \alpha_{ij})\dot{\bar{\varepsilon}}^{pl} \tag{1}$$

where $\dot{\bar{\varepsilon}}^{pl}$ is the equivalent plastic strain rate and C is the kinematic hardening modulus. In this model the equivalent stress defining the size of the yield surface, σ^0, remains constant, $\sigma^0 = \sigma\big|_0$, where $\sigma\big|_0$ is the equivalent stress defining the size of the yield surface at zero plastic strain.

The evolution law of nonlinear isotropic/kinematic hardening model consists of two components: a nonlinear kinematic hardening component, which describes the translation of the yield surface in stress space through the backstress, α; and an isotropic hardening component, which describes the change of the equivalent stress defining the size of the yield surface, σ^0, as a function of plastic deformation.

The kinematic hardening component is defined to be an additive combination of a purely kinematic term (linear Ziegler hardening law) and a relaxation term (the recall term), which introduces the nonlinearity. In addition, several kinematic hardening components (backstresses) can be superposed, which may considerably improve results in

some cases. When temperature and field variable dependencies are omitted, the hardening laws for each backstress are in Eq. (2) [16].

$$\alpha = C\frac{1}{\sigma^0}(\sigma_{ij} - \alpha_{ij})\dot{\bar{\varepsilon}}^{pl} - \gamma\alpha_{ij}\dot{\bar{\varepsilon}}^{pl} \tag{2}$$

C and γ are material parameters that must be calibrated from cyclic test data. C is the initial kinematic hardening moduli, and γ determine the rate at which the kinematic hardening modulus decreases with increasing plastic deformation.

The isotropic hardening behavior of the model defines the evolution of the yield surface size, σ^0, as a function of the equivalent plastic strain, $\bar{\varepsilon}^{pl}$. This evolution can be introduced by specifying σ^0 directly as a function of $\bar{\varepsilon}^{pl}$ in tabular form by using the simple exponential law in Eq. (3) [16].

$$\sigma^0 = \sigma\big|_0 + Q_\infty(1 - e^{-b\bar{\varepsilon}^{pl}}) \tag{3}$$

where Q_∞ and b are material parameters. Q_∞ is the maximum change in the size of the yield surface, and b defines the rate at which the size of the yield surface changes as plastic straining develops. When the equivalent stress defining the size of the yield surface remains constant ($\sigma^0 = \sigma\big|_0$), the model reduces to a nonlinear kinematic hardening model. In this paper, numerical analysis is accounted by the nonlinear isotropic/kinematic hardening model, because this model provides more accurate predictions. The parameters required by the material model were obtained from cyclic tests under strsin-control conditions. The material parameters for the kinematic hardening model were determined to be as follows: $C = 36692MPa$ and $\gamma = 193.5$, and for the isotropic material model, they have been evaluated as $Q = 217.5MPa$ and $b = 3.48$.

In numerical analysis, the boundary conditions are similar to experimental tests. Two ends of the plate are bound with rigid plate. Each rigid plate has a reference point. Reference point in the lower rigid plate with boundary condition of displacement/rotation type is bound to every direction. i.e. ($U1 = U2 = U3 = UR1 = UR2 = UR3 = 0$). The upper reference point is bound to every direction except the direction of loading. Reference point in the upper rigid plate is subjected to cyclic loading under force-controlled condition.

Element S8R5 was used in numerical simulation which is an eight node shell element with five degree of freedom in each node. Due to stress concentration around the notch, size of the elements are smaller than another area.

4 NUMERICAL RESULTS

In this section, stress and strain at notch root are attained to analyze accumulation of strain and hysteresis loops at notch root. Ratcheting strain is defined as average of maximum strain and minimum strain in each cycle.

For mechanical components subjected to cyclic loading leading to plastic strain, most materials exhibit the phenomena of mean stress relaxation or ratcheting, depending on the load conditions and structure geometry. Under force-control and displacement control conditions, ratcheting and mean stress relaxation will occur, respectively. For a component with geometrical discontinuities such as notch, neither the stress nor the strain at the notch root is under the control.

In Fig. 8, hysteresis curve at notch, which are obtained from numerical analysis for plate with notch diameter of $8mm$ under cyclic force-control loading, are shown. For the plates with circular cutouts under cyclic loading, specimens exhibit the global accumulation of plastic deformation and ratcheting phenomena but at the notch root, botch ratcheting and mean stress relaxation occur simultaneously. As ratcheting depends on the existence of a nonzero mean stress, it can be seen that the local mean stress is gradually relaxes and eventually the stress-strain loops will stabilize with a local zero mean stress and the accumulation of plastic deformation at notch root will come to stop [10].

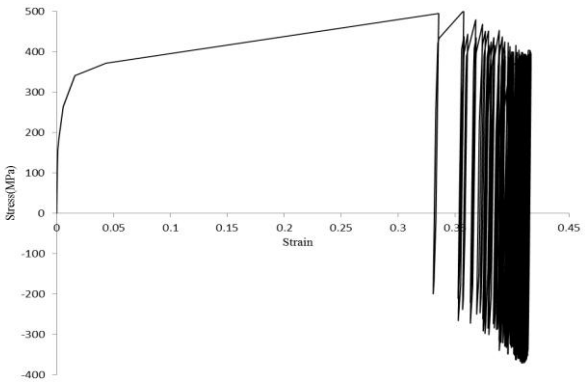

Fig. 8
Local axial stress-strain response of specimen with notch diameter of 8*mm* at notch root under cyclic axial loading in numerical results.

Fig. 9 shows the ratcheting strain at notch root versus the number of cycles for the plates with different notch diameters. As the figure shows, for a specimen, local ratcheting strain is increased whereas its rate is decreased continuously with increasing the cyclic number. Also, as said in previous, due to existence of great nominal stress in net section around the larger notch, the ratcheting displacement is higher for specimen with the larger notch. By comparing Fig. 4 and Fig. 9, it can be conclude global ratcheting is governed by the local strain and plastic deformation.

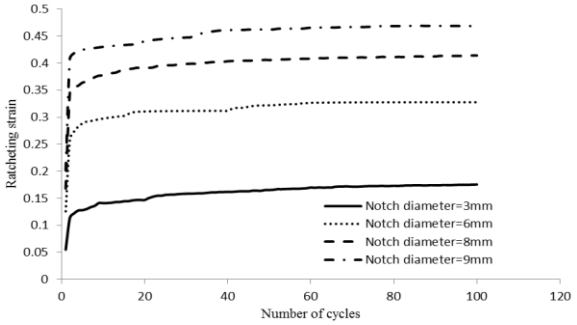

Fig. 9
Numerical local ratcheting strain for plates with different notch diameter.

5 CONFIRMATION OF NUMERICAL RESULTS WITH EXPERIMENTAL DATA

The results of experimental tests on plates with circular cutouts are compared with numerical findings in Figs. 10-13. It can be seen that the ratcheting displacement is increased, whereas its rate is decreased continuously with increasing the cyclic number in numerical results.

By comparing the experimental data with numerical results, we can see that the ABAQUS predicts appropriately in the initial cycles but after a certain cycles, except for plate with notch radius of 9*mm*, numerical method give larger ratcheting displacement under the same loading condition. Generally, there is a good agreement between experimental results and numerical results by using nonlinear isotropic/kinematic hardening model.

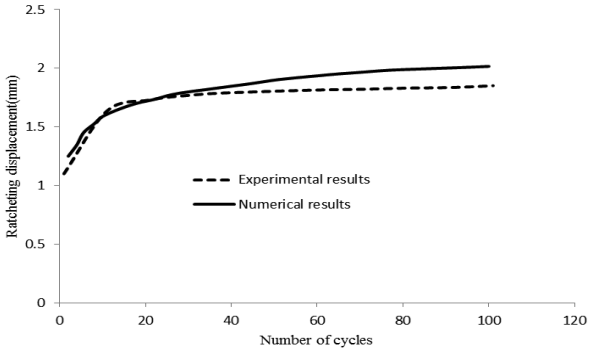

Fig. 10
Comparison of experimental and numerical ratcheting displacement for plate with notch diameter of 3*mm*.

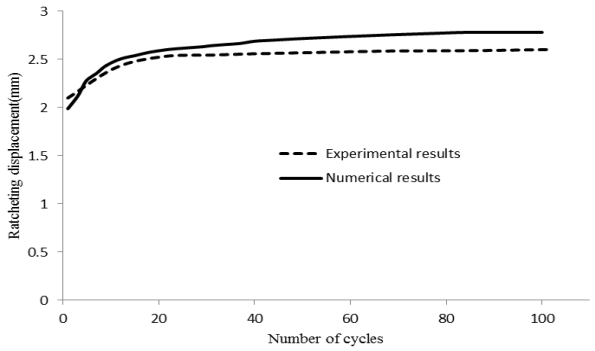

Fig. 11
Comparison of experimental and numerical ratcheting displacement for plate with notch diameter of 6*mm*.

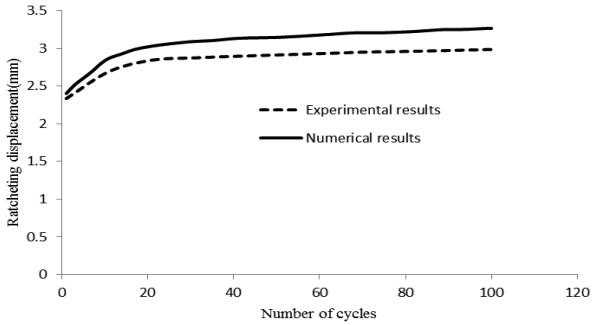

Fig. 12
Comparison of experimental and numerical ratcheting displacement for plate with notch diameter of 8*mm*.

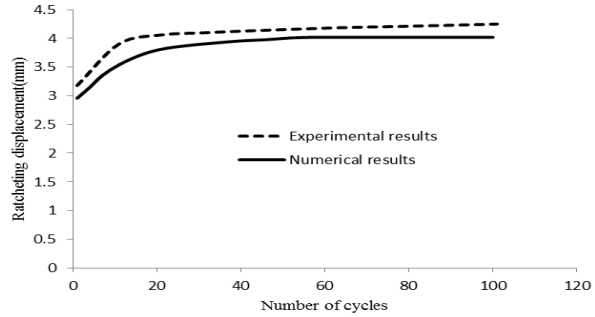

Fig. 13
Comparison of experimental and numerical ratcheting displacement for plate with notch diameter of 9*mm*.

According to numerical analysis using ABAQUS software, maximum principal stress at notch root is the highest and its value decreases by getting away from notch root on circular edge to be equal to yield stress at angle position of 39 degree with respect to the horizontal line (Fig. 14). So, maximum principal stress along the notch edge from notch root to angle position of 39 degree is higher than yield stress. Experimental observations with Dino light camera indicated that the farthest point, where the crack is initiated, has angle position lower than of 39 degree (Fig. 15). By comparing numerical results and experimental observations, the crack initiates initially at the sites where the maximum principal stress is higher than yield stress. So, maximum principal stress as a parameter for locating position of crack initiation and failure around the notch edge will be useful [11].

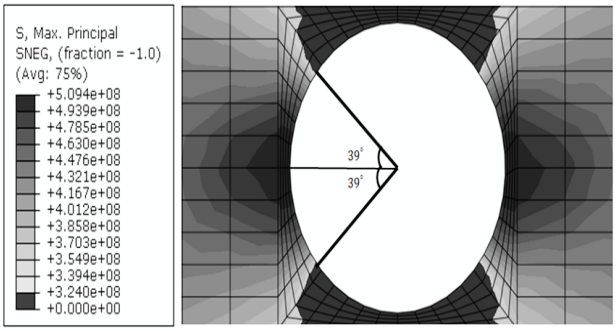

Fig. 14
Axial maximum principal stress distribution of specimen with notch diameter of 9*mm* in numerical results.

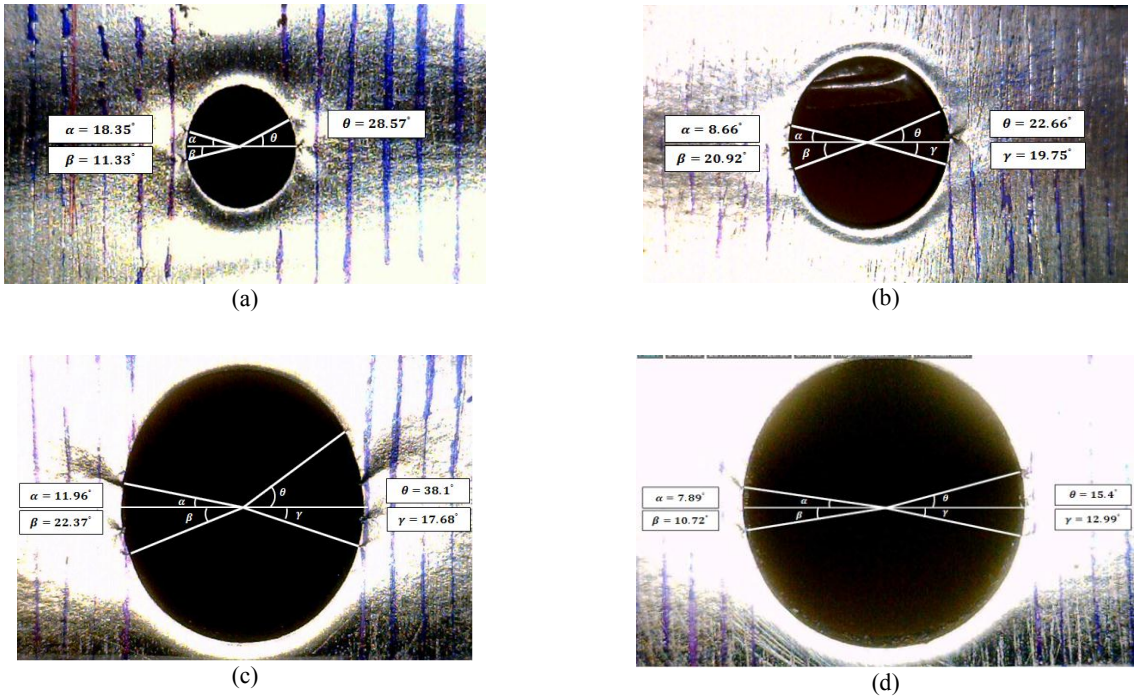

Fig. 15
Angle position of crack initiation around the notch with notch diameter of (a) 3*mm*, (b) 6*mm*, (c) 8*mm*, (d) 9*mm*, in experimental observations.

6 CONCLUSIONS

The present research discuses about ratcheting behavior of plates with circular cutouts made of AISI 1045 steel under cyclic loadings using numerical methodology and compared to experimental results. The following results were found in this study:

1. Under force-control conditions, accumulation of plastic deformation or the ratcheting phenomena occurs in the plates with circular cutouts. As the number of cycles increases, the ratcheting displacement increases while its rate fall down at first and finally increases up to failure.
2. In experimental results, for plates, by increasing of notch diameters, ratcheting displacement increases because of existence of larger nominal stress in net section around the notch.
3. The main crack around the notch growths slowly at first and gradually rate of growth increases. Also, for notch with larger diameters, the speed of crack propagation is high.
4. The existing nonlinear isotropic/kinematic hardening model in ABAQUS software simulates well the ratcheting characteristics of plates with circular cutouts and match well with the experimental results. By comparing numerical results and experimental observations, crack occurs at the locations where the maximum principal stress is the higher than yield stress.
5. In numerical analysis, local ratcheting strain at notch root is higher for notch with larger diameters. Also, the global plastic deformation is governed by local strain around the notch root under the same loading and geometric dimensions.
6. In numerical results, both ratcheting and local mean stress relaxation phenomena occur simultaneously at notch root and by increasing the number of cycles. Due to relaxation of local mean stress, local accumulation of plastic deformation come to stop.

REFERENCES

[1] Dowling E., 1998, *Mechanical Behavior of Materials*, Prentice Hall, Fourth Edition.

[2] Koe S., Nakamura H., Tsunenari T., 1978, Fatigue life estimation of notched plates based on elasto-plastic analysis, *Journal of the Society of Materials Science* **27**(300): 847-852.
[3] Sakane M., Ohnami M., 1983, A study of the notch effect on the low cycle fatigue of metals in creep–fatigue interacting conditions at elevated temperatures, *Journal of Engineering Materials and Technology* **105**(2): 75-80.
[4] Sakane M., Ohnami M., 1986, Notch effect in low-cycle fatigue at elevated temperature-life prediction from crack initiation and propagation considerations, *Journal of Engineering Materials and Technology* **108**(4): 279-284.
[5] Fatemi A., Zeng Z., Plaseied A., 2004, Fatigue behavior and life predictions of notched specimens made of QT and forged microalloyed steels, *International Journal of Fatigue* **26**: 663-672.
[6] Varvani-Farahani A., Kodric T., Ghahramani A., 2005, A method of fatigue life prediction in notched and un-notched components, *Journal of Material Processing Technology* **169**: 94-102.
[7] Medekshas H., Balina V., 2006, Assessment of low cycle fatigue strength of notched components, *Materials&Design* **27**: 132-140.
[8] Nozaki M., Zhang S., Sakane M., Kobayashi K., 2011, Notch effect on creep-fatigue life for Sn-3.5Ag solder, *Engineering Fracture Mechanics* **78**: 1794-1807.
[9] Savaidis A., Savaidis G., Zhang Ch., 2001, Elastic-plastic FE analysis of a notched shaft under multiaxial nonproportional synchronous cyclic loading, *Theoretical and Applied Fracture Mechanics* **36**: 87-97.
[10] Wang CH., Rose L.R.F., 1998, Transient and steady-state deformation at notch root under cyclic loading, *Mechanics of Materials* **30**: 229-241.
[11] Shi D.Q., Hu X.A., Wang J.K., Yu H.C., Yang X.G., Huang J., 2013, Effect of notch on fatigue behavior of a directionally solidified superalloy at high temperature, *Fatigue & Fracture of Engineering Materials & Structures* **36**: 1288-1297.
[12] ASTM A370-05, Standard test method and definitions for mechanical testing of steel products.
[13] Chen G., Chen X., Chang-Dong N., 2006, Uniaxialratchetingbehaviorof63Sn37Pb solder with loading histories and stress rates, *Material Science and Engineering A* **421**: 238-244.
[14] Shariati M., Kolasangiani K., Norouzi G., Shahnavaz, A., 2014, Experimental study of SS316L cantilevered cylindrical shells under cyclic bending load, *Thin-Walled Structures* **82**: 124-131.
[15] Gaudin C., Feaugas X., 2004, Cyclic creep process in AISI 316L stainless steel in terms of dislocation patterns and internal stresses, *Acta Materials* **52**: 3097-3110.
[16] ABAQUS 6.10.1 PR11 user's manual.